Longitude-dependent lunar tidal modulation of the equatorial electrojet during stratospheric sudden warmings

Tarique A. Siddiqui[1,2], Claudia Stolle[1,2], Hermann Lühr[1]

[1] GFZ German Research Centre for Geosciences, Potsdam, Germany
[2] Institute of Earth and Environmental Science, University of Potsdam, Germany
contact – tarique@gfz-potsdam.de

CEDAR Workshop - 2017

Introduction

Stratospheric Sudden Warmings

- Stratospheric Sudden Warmings (SSWs) are large-scale meteorological events usually occurring during the northern hemisphere winters. SSW was first observed by Richard Scherhag in 1952 at the Free University of Berlin and was initially termed as the “Berlin phenomenon”.
- SSWs are characterized by a weakening or sometimes even a reversal of the westerly winds in the northern stratosphere that leads to a sudden rise in polar stratospheric temperature by several tens of degrees.
- The underlying mechanism behind SSWs is understood to be the nonlinear interaction of the vertically propagating planetary waves with the zonal mean flow (Matsuno, 1971).

The 2009 SSW event

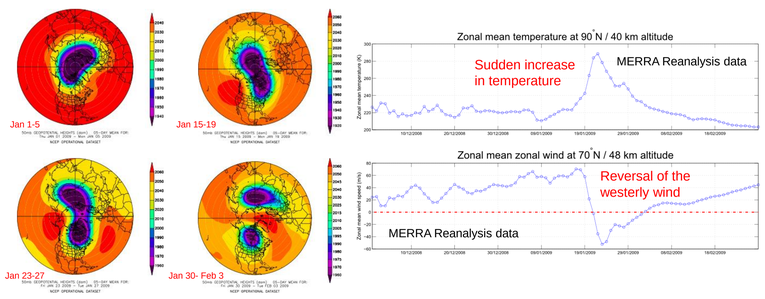

The left part of the figure presents the composite of 50 mb geopotential heights (dam) for the above-mentioned dates and shows the splitting of the polar vortex during the 2009 SSW event. The plots are downloaded from https://www.esrl.noaa.gov. The right part of the figure shows the temperature at North Pole at 40 km altitude and the zonal mean zonal wind at 70°N and 48 km altitude during Dec 2008 – Feb 2009 from the MERRA reanalysis data set.

SSW related impacts in the atmosphere

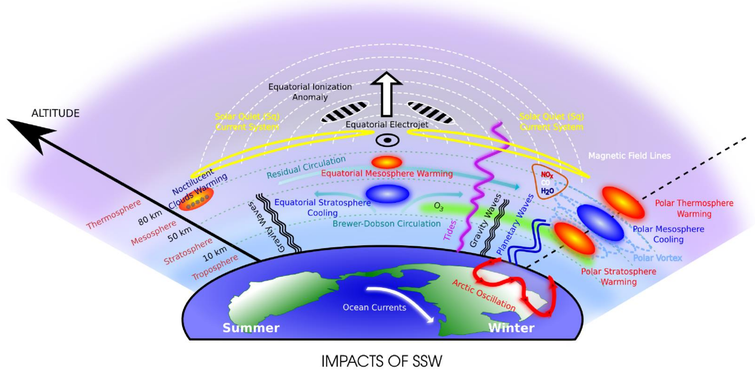

The schematic shows the known impacts of SSW in the atmosphere (Figure adapted from Pedatella et al., 2017 (submitted to Eos).

Equatorial Electrojet

- The equatorial electrojet (EEJ) is a narrow band of an intense electric current confined to a latitude band of about ±3° and flowing above the magnetic dip equator at an altitude of around 110 km in the daytime E-region of the ionosphere.
- The primary reasons for the high current densities at these latitudes can be attributed to the horizontal geometry of geomagnetic field lines and the Cowling effect that leads to regions of enhanced conductivities over the dip equator.

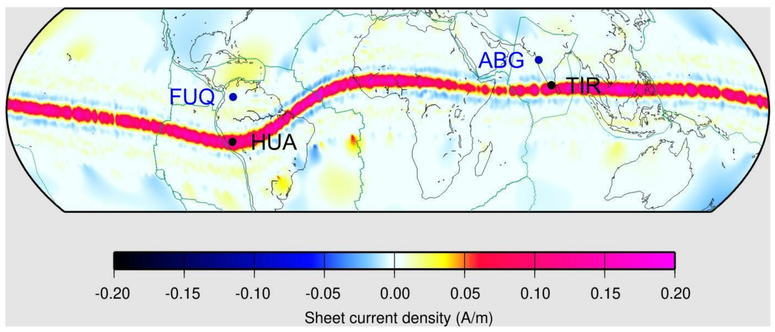

Electrojet current densities inferred from 2600 passes of the CHAMP satellite over the magnetic equator between 11:00 and 13:00 local time (Figure is from http://geomag.org/info/equatorial_electrojet.html). The location of the observatories used in this work has been marked with dots.

Methods of Analysis

Estimating lunar tidal amplitude from:

Ground magnetic recordings

$H = H_{MF} + H_{MP} + H_{EEJ} + H_{Sq}$

H_{MF} - Earth's main magnetic field
H_{MP} - Field due to magnetospheric currents
H_{EEJ} – Field due to equatorial electrojet
H_{Sq} – Field due to Sq current system

$\Delta H = H - H_{MF}$

H_{MF} estimated from quiet-nighttime values

$H_{EEJ} = \Delta H_{HUA/TIR} - \Delta H_{FUQ/ABG}$

H_{EEJ} normalized to solar flux level of 150 s.f.u. The dominant solar tidal variations are removed by subtracting the means over a 59-day moving window for each local time.

Amplitude and phase of the semi-monthly lunar tide is calculated for 08:00-16:00 LT using FFT for each 59-day moving window. The mean amplitude over all LTs is then determined.

CHAMP magnetometer measurements

$$EEJ' = \frac{EEJ}{\sqrt{\frac{F_{10.7p}}{150} \times \left| cos\frac{\pi}{12}(LT - 12\ h) \right|}}$$

Normalization of EEJ peak intensity

EEJ' is computed for:
Peruvian Sector - 235° - 325°E
Indian Sector - 45° - 135°E

A 39-day moving window is selected due to the periodicity of M_2 tide from the CHAMP satellite frame being 13.26 days and the M_2 amplitude is then estimated using FFT.

SABER temp. measurements

Periodicity of M_2 from TIMED satellite frame is 11.85 days. M_2 tide determined from SABER temperature measurements within ±5° latitude around HUA & TIR.

A 12-day running window is used to calculate the residuals after removing the background temperature. Residuals are then fitted with a sinusoidal function using least-squares method to estimate the M_2 amplitude.

Observations and Results

2006 SSW event

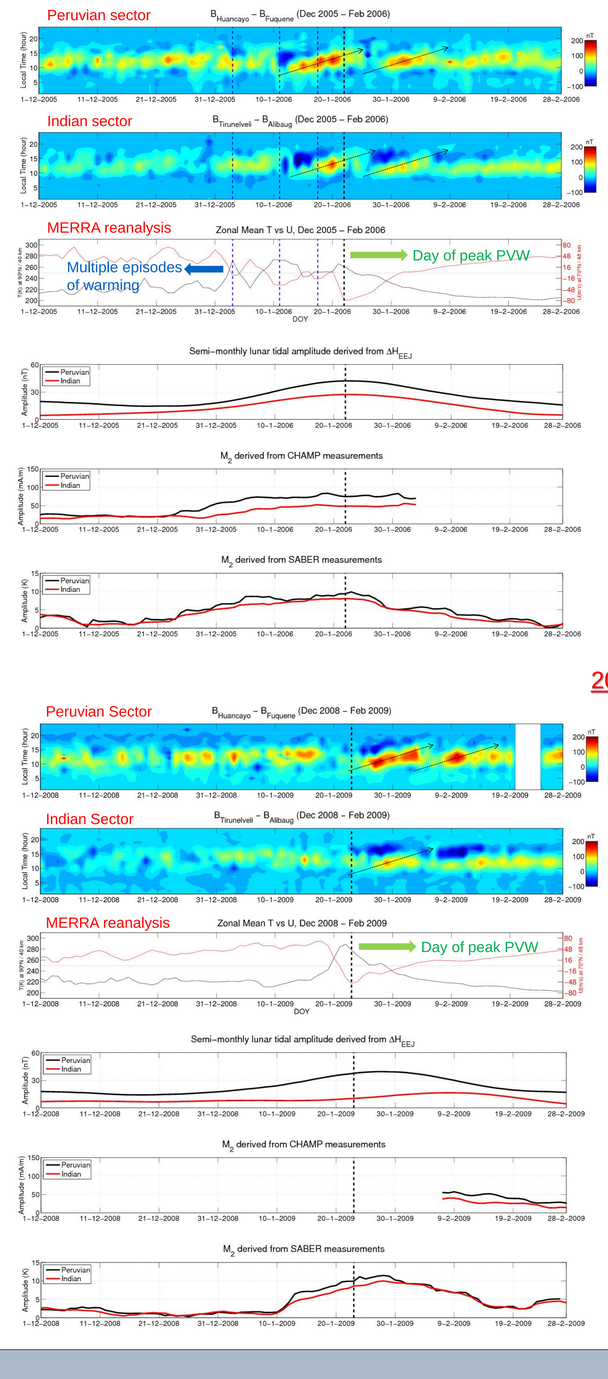

Arrows represent the lunar tidal modulation of EEJ during SSW.

Strong lunar tidal modulation of EEJ during SSW is seen in both the sectors after the peak day of polar vortex weakening (PVW). The time - shifting semi-diurnal perturbation pattern is clearly observed in both the sectors.

The timing of lunar tidal enhancement in EEJ is similar in both the sectors.

M_2 amplitude derived from SABER temp. measurements shows lesser longitudinal variability as compared to lunar tidal amplitudes in EEJ.

2009 SSW event

Arrows represent the lunar tidal modulation of EEJ during SSW.

Lunar tidal modulation of EEJ starts a few days after the day of peak PVW and the semi-diurnal perturbation pattern is clearly seen only in the Peruvian sector.

Modulation of EEJ is weaker in the Indian sector.

Compared to the day of peak PVW, the timing of lunar tidal enhancement in EEJ is delayed in the Indian sector.

M_2 amplitude derived from SABER temp. measurements again shows lesser longitudinal variability as compared to lunar tidal amplitudes in EEJ.

Results continued…

2006-2007 non-SSW winter

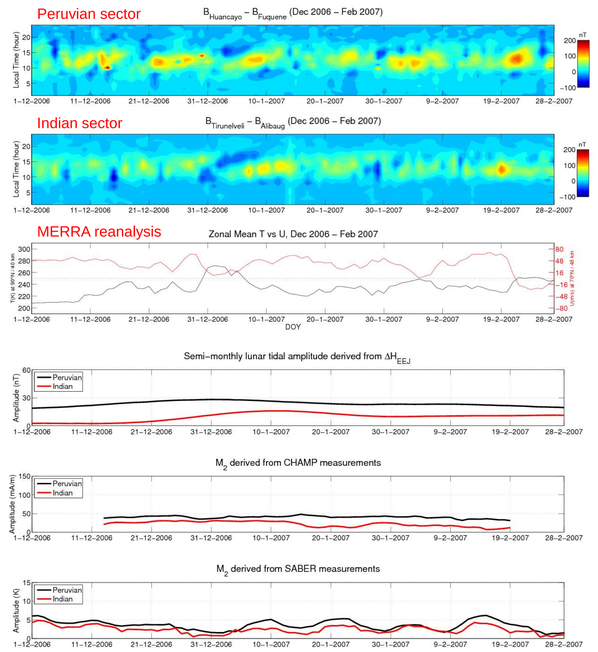

Weak modulation of EEJ is seen in both the sectors during this period.

Semidiurnal perturbation patterns are seen in both the sectors when the zonal mean wind comes close to reversal.

Reversal of the zonal mean zonal wind was not observed during this period.

Weak lunar tidal enhancements is seen in both the sectors compared to SSW periods.

M_2 amplitudes derived from CHAMP also do not show any definite enhancement.

M_2 amplitudes derived from SABER are twice as small as compared to SSW periods.

Climatological analysis of the lunar semi-monthly tide

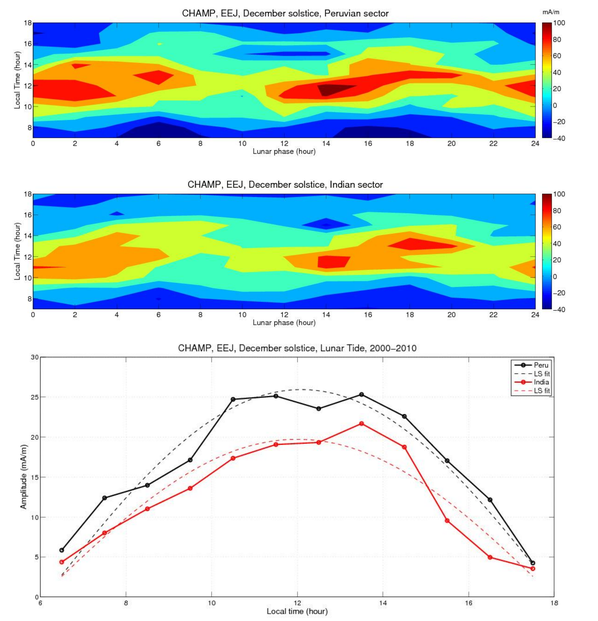

Peak EEJ current densities from the CHAMP satellite between 2000 -2010 during December solstice are sorted into bins of 2h in moon phase and 1 h in local time for both the Peruvian and Indian sectors.

EEJ intensity in the Peruvian sector is clearly larger than in the Indian sector.

Comparison of the diurnal variation of the lunar tidal amplitude in the Peruvian and Indian sectors during December solstice. The peak lunar tidal amplitude over the Peruvian sector is 1.31 times greater than over the Indian sector.

Conclusions

- Our results show the difference in lunar tidal enhancements in both the sectors during two major SSWs and a non-SSW winter. It is observed that there is a significant lunar tidal enhancement in ground- and space-based measurements during a major SSW event in comparison to a winter without a SSW event.
- Major longitudinal variabilities in lunar tidal enhancements in EEJ in the Peruvian and Indian sectors are seen during the 2009 SSW event. The semi-monthly lunar enhancements in the Indian sector are much smaller and occur later than in the Peruvian sector.
- During the 2009 SSW event, the M_2 amplitudes derived from SABER temperature measurements in both the sectors show similar enhancement timings, which is widely different from the enhancement of lunar semi-monthly amplitudes in EEJ during the same period. The M_2 amplitudes from SABER measurements were estimated using the daily temperature means between 00-24 LT. We suggest that the reason for the weaker and delayed lunar tidal amplitudes in EEJ over the Indian sector during this period could be due to some daytime physical processes in the E-region.

Related Papers

- Chau, J. L., L. P. Goncharenko, B. G. Fejer, and H.-L. Liu (2012), Equatorial and low latitude ionospheric effects during sudden stratospheric warming events, *Space Sci. Rev.*, *168*(1–4), 385–417.
- Forbes, J. M., and X. Zhang (2012), Lunar tide amplification during the January 2009 stratosphere warming event: Observations and theory, *J. Geophys. Res.*, *117*, A12312, doi:10.1029/2012JA017963
- Scherhag, R. (1952), Die explosionsartigen stratosphärenerwärmungen des spätwinters 1951/52, *Ber. des Dtsch. Wetterdienstes in der US-Zone*, *6*(38), 51–63.
- Matsuno, T. (1971), A dynamical model of the stratospheric sudden warming, *J. Atmos. Sci.*, *28*(8), 1479–1494.
- Maute, A., M. E. Hagan, V. Yudin, H.-L. Liu, and E. Yizengaw (2015), Causes of the longitudinal differences in the equatorial vertical $E \times B$ drift during the 2013 SSW period as simulated by the TIME-GCM, *J. Geophys. Res. Space Physics*, *120*(6), 5117–5136, doi:10.1002/2015JA021126.
- Pedatella, N., J. Chau, H. Schmidt, L. Goncharenko, C. Stolle, K. Hocke, V. Harvey, B. Funke and T. A. Siddiqui, The far-flung effects of sudden stratospheric warmings. (submitted to Eos)
- Siddiqui, T. A., C. Stolle, H. Lühr, and J. Matzka (2015), On the relationship between weakening of the northern polar vortex and the lunar tidal amplification in the equatorial electrojet, *J. Geophys. Res. Space Physics*, *120*(11), 10,006–10,019, doi:10.1002/2015JA021683.
- Siddiqui, T. A., C. Stolle, and H. Lühr (2017), Longitude-dependent lunar tidal modulation of the equatorial electrojet during stratospheric sudden warmings, *J. Geophys. Res. Space Physics*, *122*, doi:10.1002/2016JA023609.